

APPLYING VARIOUS TRAINING ALGORITHMS IN DATA ANALYSIS OF NANO COMPOSITES

Ali Asghar Tofigh¹⁾, Mohsen Ostad Shabani^{1)*}

¹⁾Materials and Energy Research Center (MERC), Tehran, Iran

Received: 09.03.2012

Accepted: 26.11.2012

*Corresponding author: e-mail: vahid_ostadshabany@yahoo.com, Tel: +98 912 563 6709, Fax: +98 261 6201888, Materials and Energy Research Center (MERC), Tehran, Iran

Abstract

In this study, SiC nano-particles were incorporated into the A356 aluminum alloy to fabricate metal matrix nano composites (MMNCs) with uniform reinforcement distribution. The tribological and mechanical properties of A356 nano composites were experimentally investigated. It was revealed that the presence of nano-SiC reinforcement led to significant improvement in hardness, 0.2% yield strength and UTS. The highest yield strength and UTS was obtained by 3.5 vol. % of SiC nano-particles. The wear sliding test disclosed that the wear resistance of the nano SiC reinforced composites is higher than that of the unreinforced alloy. The system accuracy of each artificial neural network training algorithm in finite element technique modeling of nano composites behaviors was then investigated.

Keywords: composites, wear, casting, mechanical properties

1 Introduction

Important AMC applications in the ground transportation (auto and rail), thermal management, aerospace, industrial, recreational and infrastructure industries have been enabled by functional properties that include high structural efficiency, excellent wear resistance, and attractive thermal and electrical characteristics [1-3]. While in composites reinforced with continuous fibers, strengthening is associated with load transfer from the matrix to the fiber, it is associated with the high dislocation density in the matrix of composites reinforced with whisker and particulate [4-7].

Micro size Ceramic powders and fibers were widely used in fabrication of Al-based composites to improve the ultimate tensile and the yield strengths of the metal. However, the ductility of the MMCs deteriorates significantly with high ceramic particle concentration. It will be attractive to produce as-cast lightweight bulk components of MMNCs with uniform reinforcement distribution and structural integrity. It is expected that the strength of aluminum reinforced by ceramic nano-particles, would be enhanced considerably, while the ductility of the aluminum matrix is retained. However, it is extremely difficult to obtain uniform dispersion of nano-sized ceramic particles in liquid metals due to high viscosity, poor wettability in the metal matrix, and a large surface-to-volume ratio [6-9].

Experimental results showed a relatively uniform distribution of nano particles and more than 50% improvement in yield strength of A356 alloy only with 2.0 wt. % of nano-sized SiC particles.

Zhao et al. [2] characterized the properties and deformation behavior of (Al₂O₃+Al₃Zr) np/Al nano-composites produced by magneto-chemical melt reaction. It is reported that elongation,

ultimate tensile strength and yield strength of nano-composites are enhanced with increasing of particulate volume fraction, and are markedly higher than that of Al composites synthesized by micro size particles.

ANN theory has been developed in the form of parallel distributed network models based on biological learning process of the human brain. There are numerous applications of ANN in data analysis, pattern recognition and adaptive control. In recent years, there has been a growing interest in applying artificial neural networks, a branch of modern information technology, to engineering fields for solving various complex problems [10-16]. In this paper, the mechanical and tribological properties of A356 composite reinforced with nano SiC particulates were first experimentally investigated and then the combination of FEM with ANN is implemented for modeling of these properties. The results have shown that Bayesian regularization learning algorithms gave the best result for this study.

2 Experimental conditions

Commercial casting aluminum alloy (A356) was selected as the matrix due to its good castability. The chemical composition of A356 is follows: (wt.%): 7.5 Si, 0.42 Mg, 0.03 Zn, 0.01 Cu, 0.106 Fe and Al (balance). A mixture of nano-SiC and aluminum particles with respectively average particle size of 50 nm and 16 μm was used as the reinforcement. Magnesium additive in powder form was also used as a wetting agent. The addition of 1 wt. % magnesium to the melt promote wetting by reducing the surface tension of the melt, decreasing the solid-liquid interfacial energy of the melt, or inducing wettability by chemical reaction. A stir casting setup consisting of a resistance furnace and a stirrer assembly was used for synthesizing the composites. The aluminium ingot was placed in a graphite crucible and heated to 750°C (above the alloy liquidus temperature) using the resistance furnace. Then the step casting was poured into the CO₂-sand mould. There is a nitrogen supply to the crucible in order to minimize the oxidation of molten aluminum.

The porosities of the produced composites were evaluated from the difference between the expected and the observed density of each sample. To study the hardness, the Brinell hardness values of the samples were measured on the polished samples using a ball with 2.5mm diameter at a load of 31.25 kg. The dry sliding wear test was carried out with sliding distance of 2000 m and under the load of 10 N. At least three wear samples were tested for each specimen. The slider disc was case hardened steel with 63 HRC to a depth of 3 mm. Composite were made into pin having 6 mm in diameter and 25 mm in height. The pins were put in contact with the slider. The pins were cleaned thoroughly by ultrasonic prior and after the tests with acetone and then were weighed using an electronic balance with an accuracy of 0.1 mg. All tests were performed at room temperature (21 °C, relative humidity 55%).

The tensile specimens were machined from composite rods according to ASTM.B 557 standard. For each volume fraction of SiC particles, three samples were tested. The composite rods were machined to compressive specimens with a diameter of 12 mm and height of 18 mm (height/diameter=3/2). Compression tests were conducted using a Universal Testing Machine (Schimadzu) at the strain rate of 10⁻³ and room temperature.

3 Cooling rate and temperature gradient

The numerical model is applied to simulate the solidification of alloys, the mathematical formulation of this solidification problem is given [17]:

$$\rho C \frac{\partial T(x, y, z, t)}{\partial t} = K \nabla^2 T(x, y, z, t) + \rho L \frac{\delta f_s}{\delta t} \quad (1)$$

Where ρ the density (kg/m^3), C the specific heat (J/kg K), T the temperature (K), t the time (s), K is the thermal conductivity (W/m K), L is the latent heat (J/kg) and f_s the local solid fraction. The fraction of solid in the mushy zone is estimated by the Scheil equation, which assumes perfect mixing in the liquid and no solid diffusion. With the liquidus and solidus having constant slopes, f_s is then expressed as:

$$f_s = 1 - \left(\frac{T_f - T}{T_f - T_{liq}} \right)^{1/(k_0-1)} \quad (2)$$

Where T_f is the melting temperature (K), T_L the liquidus temperature (K), and k_0 the partition coefficient. Then [17]:

$$\frac{\delta f_s}{\delta t} = \frac{1}{(k_0 - 1)(T_f - T_{liq})} \left(\frac{T_f - T}{T_f - T_{liq}} \right)^{(2-k_0)/(k_0-1)} \frac{\delta T}{\delta t} \quad (3)$$

The latent heat released during solidification of the remaining liquid of eutectic composition was taken into account by a device, which considers a temperature accumulation factor.

$$\rho C' \frac{\partial T(x, y, z, t)}{\partial t} = K \nabla^2 T(x, y, z, t) + \rho L \frac{\delta f_s}{\delta t} \quad (4)$$

Where C' can be considered as a pseudo-specific heat given by:

$$C' = C_M - L \frac{\delta f_s}{\delta T} \quad (5)$$

$$C_M = (1 - f_s)C_l + f_s C_s \quad (6)$$

Where the subscripts L, S and M refer to liquid, solid and mushy, respectively. The other properties such as thermal conductivity and density in the mushy zone are described similarly as the specific heat:

$$K_M = (1 - f_s)K_l + f_s K_s \quad (7)$$

$$\rho_M = (1 - f_s)\rho_l + f_s \rho_s \quad (8)$$

The finite element method (FEM) was used for discretization. Based on the above transient temperature model, the FEM method is used to calculate the transient temperature, cooling rate and temperature gradient.

4 Neural network training algorithms

The neural network modelling and simulation procedures implemented in this paper were done in five steps as follows:

- data collection

- pre-processing of collected data
- neural network training
- testing of the trained neural network model
- predictive simulations using the trained neural network models.

Various training algorithms can be utilized in neural network applications. It is hardly difficult to predict which of these learning will be the fastest one for any problem. Generally, it depends on some factors; the structure of the networks, in other words, the number of hidden layers, weights and biases in the network, aimed error at the learning, and application area, for instance, pattern recognition or classification or function approximation problem [1, 11]. However, the data structure and uniformity of the training set are also important things that affect the system accuracy and performance. Some of famous train algorithms are as follow [18-28]:

- Bayesian regularization: is a network training function that updates the weight and bias values according to LM optimization. It minimizes a combination of squared errors and weights, and then determines the correct combination so as to produce a network that generalizes well. The process is called Bayesian regularization.
- Batch unsupervised weight/bias training: trains a network with weight and bias learning rules with batch updates. Weights and biases updates occur at the end of an entire pass through the input data.
- Cyclical order incremental update: trains a network with weight and bias learning rules with incremental updates after each presentation of an input. Inputs are presented in cyclic order.
- Powell-Beale conjugate gradient back propagation: is a network training function that updates weight and bias values according to the conjugate gradient back propagation with Powell-Beale restarts.

After satisfactory training, the neural network models were used for further simulations and predictions of different correlations and phenomena in processing-structure-properties relationships. In the analysis of performance of various training algorithms, the same prepared learning and test set were used in the training processes of each learning algorithm. The performance analysis were done from the viewpoint of training duration, error minimization and prediction achievement. The ANN predictions were directly compared with the experimental obtained data to evaluate the learning performance. Mean absolute percentage error (MAPE), which is statistical and scientific error computation method, was used to analyze the error.

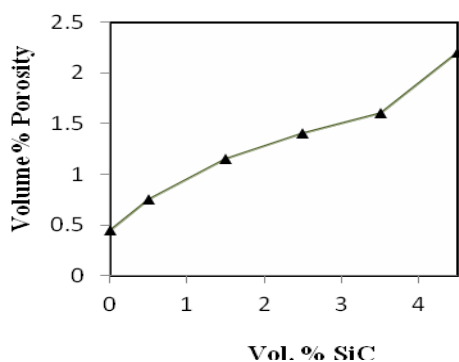


Fig.1 Variations of porosity with Vol. % SiC

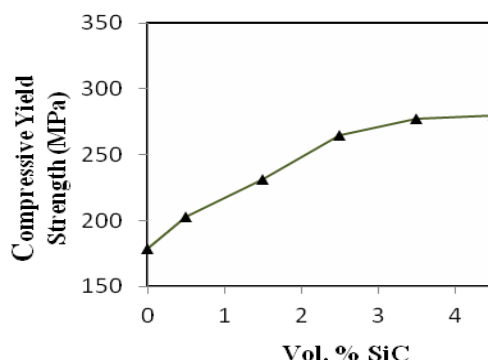


Fig.2 Compressive yield strength with Vol. % SiC

5 Results and discussion

Comparison of the measured density of the cast alloy and the composites with that of their theoretical density determined the amount of porosity. **Fig. 1** indicates that increasing amount of porosity is observed with increasing the volume fraction of composites. The porosity level increased, since the contact surface area was increased. In the other word, higher degree of defects and micro-porosity is observed at composites with higher SiC content which is the result of increase in the amount of interface area [9, 29, 30].

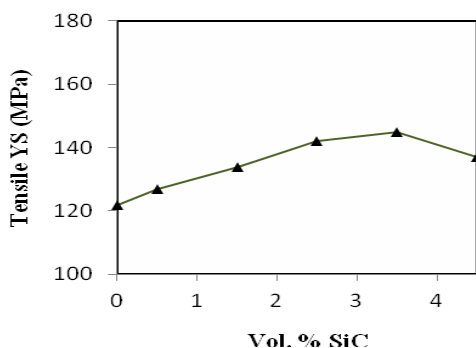


Fig. 3 Tensile yield strength versus vol. % SiC

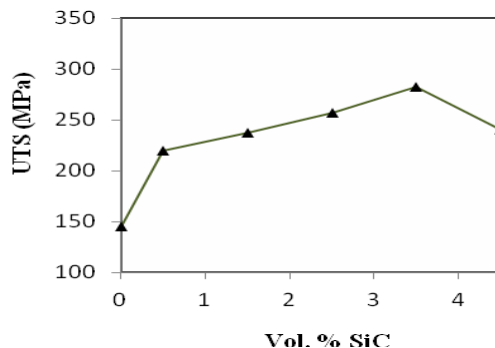


Fig. 4 The UTS versus vol. % SiC

Figs. 2, 3 and 4 display compressive yield strength, tensile yield strength and UTS of the composites, respectively. It is believed that the great enhancement in compressive and tensile strength observed in these composites is due to good distribution of the nano-SiC particles and low degree of porosity which leads to effective transfer of applied tensile load to the uniformly distributed strong SiC particulates. The grain refinement and strong multidirectional thermal stress at the Al/SiC interface are also important factors, which play a significant role in the high strength of the composites. SiC particles have grain-refined strengthening effect, since they act as the heterogeneous nucleation catalyst for aluminum which is improved with increase in the volume fraction [9, 31-33].

The difference between the coefficient of thermal expansion (CTE) values of matrix and ceramic particles generates thermally induced residual stresses and increases dislocations density upon rapid solidification during the fabrication process. The interaction of dislocations with the non-shearable nano-particles increases the strength level of composite samples. According to the Orowan mechanism, the nano-SiC particles act as obstacles to hinder the motion of dislocations near the particles in the matrix. This effect of particles on the matrix is enhanced gradually with the increase of particulate volume fraction [2, 31].

According to the results of this experiment, quite significant improvement in tensile strength is noted initially when particles are added; however, further increase in SiC content leads to reduction in strength values. The weakening factors of mechanical properties might be responsible for this including particles clusters and porosity. Hereby, it is believed that strengthening and weakening factors of mechanical properties could neutralize the effect of each other and thus, the composite containing 3.5 vol. % SiC exhibits maximum tensile strength. The thermal mismatch residual stress generated due to difference in the thermal expansion coefficients between the matrix alloy and the reinforcing phase is believed to enhance the compressive property more than tensile property of composite. This might be the reason that though the maximum tensile flow stress is observed at 3.5 vol. % SiC, increasing volume fraction from 3.5 to 4.5 vol. % leads to increment in compressive flow stress [9, 31].

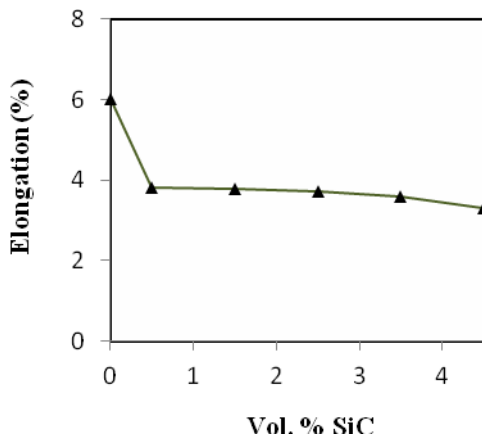


Fig. 5 Elongation versus vol. % SiC

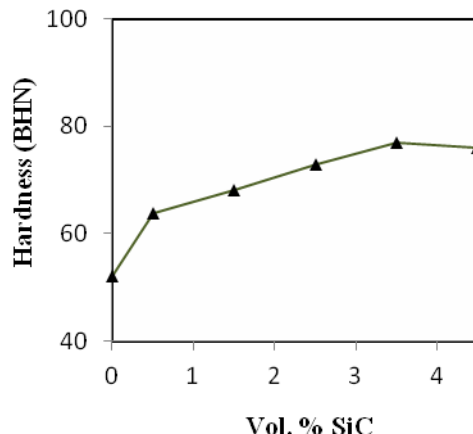


Fig. 6 The hardness versus vol.% SiC

Normally micron-sized particles are used to improve the ultimate tensile and the yield strengths of the metal. However, the ductility of the MMCs deteriorates significantly with high ceramic particle concentration [35-37].

Fig.5 shows that the addition nano-particles deteriorates the ductility of A356 alloy. The stir casting method that is used in the present work to produce the nano-composites can most probably create different interfaces between nano-particles and matrices and thus, encourage crack initiation and propagation [38]. It is also noted that the elongation remain rather constant with the addition of nano particles. This is consistent with the findings of Hassan and Gupta [39, 40].

The results of hardness for Al/nano-SiC composites are summarized in **Fig. 6**. It is clear from the graph that the hardness of the composites is higher than that of the non-reinforced alloy. The higher hardness of the composites could be attributed to the fact that SiC particles act as obstacles to the motion of dislocation. The hardness increment can also be attributed to reduced grain size. As shown, hardness increases with the amount of SiC present particles. It is believed that since SiC particles are harder than aluminum alloy, their inherent property of hardness is rendered to the soft matrix [32, 33].

The weight loss versus sliding distance of the specimens is shown in **Fig. 7**. It is clear that the weight loss has a declining trend with increasing the particles volume fraction. This result is consistent with the rule that in general, materials with higher hardness have better wear and abrasive resistance [41].

The results show that the wear of the composites decreases with increasing SiC volume fraction. It is generally believed that incorporation of hard particles to aluminum alloys contributes to the improvement of the wear resistance of the base alloy to a great extent [42]. SiC hard particles resist against destruction action of abrasive and protect the surface, so with increasing its content, the wear resistance enhances but it seems this enhancement continues until the reinforcement can improve the mechanical properties such as hardness e.g. in case of nano-sized particle clustering, the trend of wear resistance improvement may be affected by the particle agglomeration.

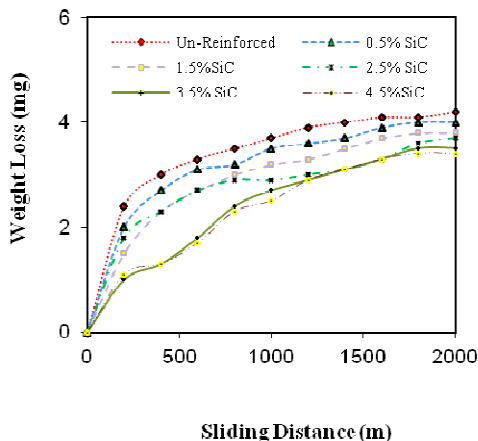


Fig. 7 The weight loss versus sliding distance

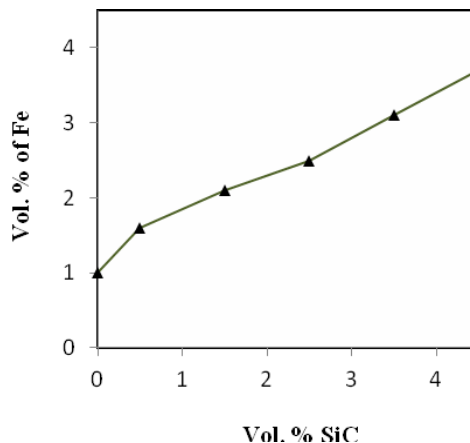


Fig. 8 The Fe content on the worn surfaces.

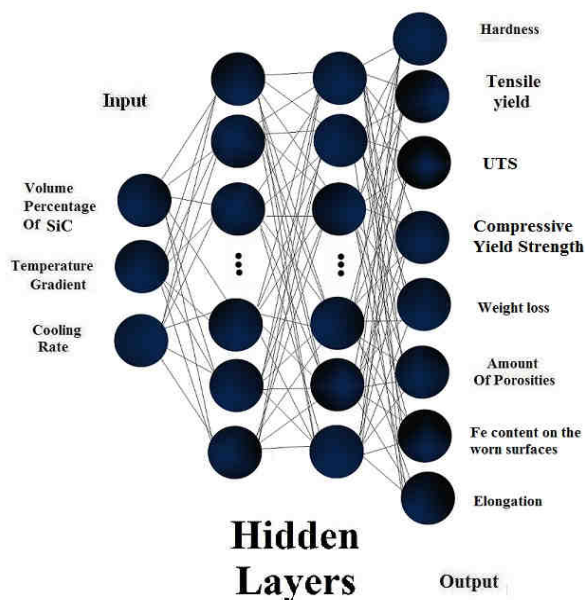


Fig. 9 Schematic representation of the neural network architecture

In the composite, the reinforcement particles support the Load, decrease the contact area between the pin and counter disc surface and prevent the scratch and cut from the surface [43]. This is probably the main reason for the observed enhancement in wear resistance of the composite.

Some researchers have shown that for loads below 10 N, Al_2O_3 and SiC reinforcement increased the wear resistance of Al and Mg alloy matrix composites due to the load bearing capacity improvement of the particulates and the formation of a transfer layer which protect the surface from abrasion [41, 44]. Fig. 8 shows the Fe content variation on the worn surface with SiC content. It is observed that the formation of iron-rich layers on the contact surfaces increases with increasing the SiC content.

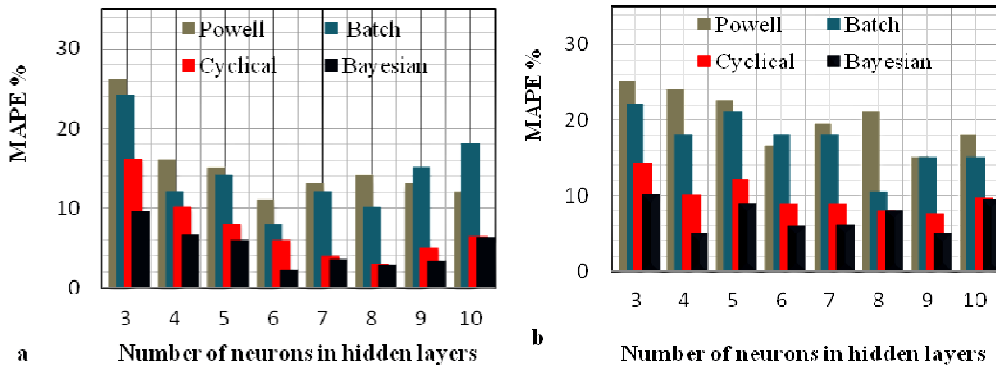


Fig. 10 Evaluation of the training performance of the networks for different training algorithms according to mean absolute percentage error values with, one hidden layer (a), two hidden layers (b)

The input and output data set of the model is illustrated schematically in **Fig. 9**. In **Fig. 10**, obtained mean absolute percentage error (MAPE) values for training data were given for each training algorithm. The obtained error values for different number of neurons in the hidden layers and number of hidden layers were analyzed and given, graphically. This figure also gives information about the accuracy of four famous training algorithms depending on the number of neurons in the hidden layers and number of hidden layers. It is evident from this figure; the least error value was obtained by using Bayesian regularization training algorithm with 1 hidden layer and 6 neurons. Cyclical order incremental update with 1 hidden layer and 8 neurons in the hidden layers follows Bayesian regularization training algorithm. Normally for most problems one hidden layer would be good enough. Using more than one hidden layer actually does not lead to a good model as they are very likely to over fit the data. The much error was obtained from the Batch unsupervised weight/bias training and Powell-Beale conjugate gradient back propagation. The Bayesian regularization was found to be the fastest training algorithm, however it requires more memory with the same error convergence bound compared to training methods. MAPE is a good criterion to have information about learning performance. The iterations were continued until it is decided that the minimum MAPE error is obtained.

In addition, success in the algorithms depends of the user dependent parameters learning rate and momentum constant. Faster algorithms such as Bayesian regularization use standard numerical optimization techniques. These algorithms eliminate some of the disadvantages above mentioned. Bayesian regularization method is in fact an approximation of the Newton's method. The algorithm uses the second order derivatives of the cost function so that a better convergence behavior can be obtained. In the ordinary training method, only the first-order derivatives are evaluated and the parameter change information contains solely the direction along which the cost is minimized, whereas the Bayesian regularization technique extracts a better parameter change vector.

Fig. 11 shows the efficacy of the optimization scheme by comparing the prediction results with the experimental values. There is a convincing agreement between experimental values and predicted values for elongation and weight loss of nano composite for Bayesian regularization training algorithm.

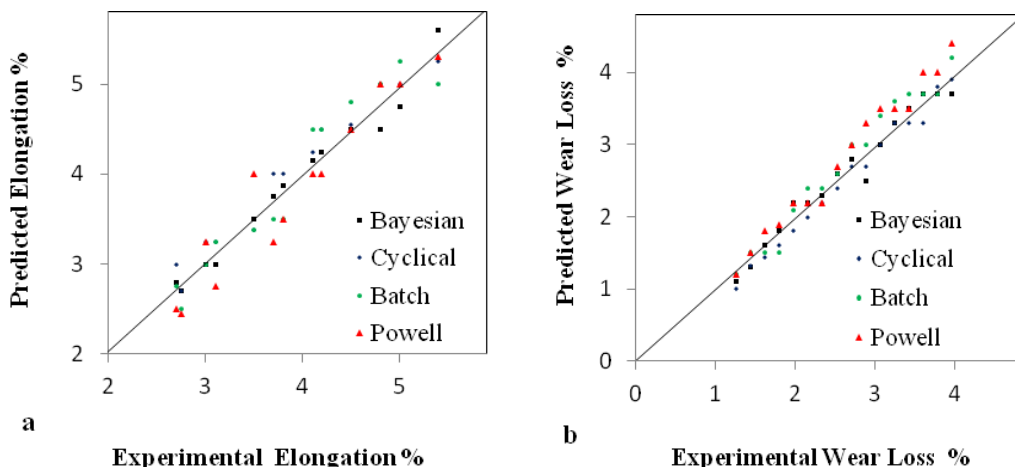


Fig. 11 Comparison between the experimental and predicted values: Elongation (a) and Weight loss (b)

6 Conclusion

The effects of SiC reinforcement on hardness, tensile, compressive and wear properties of the composites were investigated. The addition of nano-particles also resulted in significant improvements in wear of the composites. Different strengthening mechanisms contributed in improvements of tensile and compressive behavior of the composites including Orowan strengthening, grain refinement, accommodation of CTE mismatch between the matrix and the particles, and the load bearing effects. Tribological and mechanical properties are considered to be related to cooling rate, temperature gradient and volume percentage of nano-SiC particles. The FEM method is used for discretization and to calculate the transient temperature field of quenching. It is very difficult to generalize which training algorithm of the neural network will be the fastest one and can present a very good performance for any given problem. However the results of this study show that an ANN with 6 neurons in 1 hidden layers with Bayesian regularization method give the best properties prediction of nano composites.

Reference

- [1] M. O. Shabani, A. Mazahery: Applied Mathematical Modeling, Vol. 35, 2011, p. 5707–5713
- [2] A. Mazahery, M. O. Shabani: Ceramics Internationals, Vol. 38, 2012, p. 4263-4269
- [3] S.F. Hassan, E. Gomes: Computers and Structures, Vol. 23, 2005, p. 2253–2258
- [4] H. Ferkel, B.L. Mordike: Material Science and Engineering A, Vol. 298, 2001, p. 193–199.
- [5] J.R. Groza: International Journal Powder Metallurgy, Vol. 35, 1999, p. 59–66
- [6] M. O. Shabani, A. Mazahery: Applied Mathematical Modeling, Vol. 36, 2012, p. 5455–5465
- [7] J. Lan, Y. Yang, X. Li: Materials Science and Engineering A, Vol. 386, 2004, p. 284–290
- [8] J. Lan, Y. Yang, X. Li: Materials Science and Engineering A, Vol. 380, 2004, p. 378-383
- [9] A. Mazahery, M. O. Shabani: Ceramics International, Vol. 38, 2012, p. 1887–1895.
- [10] K. Elangovan, C. S. Narayanan, R. Narayanasamy: Composite Materials Science, Vol. 47, 2010, p. 1072–1078

- [11] M. O. Shabani, A. Mazahery: *Metallurgical and Materials Transactions A*, Vol. 43, 2012, p.2158-2165
- [12] A.M. Rashidi, A.R. Eivani, A. Amadeh: *Composite Materials Science*, Vol. 45, 2009, p. 499–504
- [13] R. Koker, N. Altinkok, A. Demir: *Materials and Design*, Vol. 28, 2007, p. 616–627
- [14] T. Wen, L. Z. Yu, W. Di, W. G. Dong: *Journal of Iron and Steel Research*, Vol. 16, 2009, p. 80-83
- [15] Z. Sterjovski, D. Nolan, K.R. Carpenter, D.P. Dunne, J. Norrish: *Journal of Materials Processing and Technology*, Vol. 170, 2005, p. 536–544
- [16] S.H. M. Anijdan, A. Bahrami, H.R. M. Hosseini: *Materials and Design*, Vol. 27, 2006, p. 605–609
- [17] A. Mazahery, M. O. Shabani: *Powder Technology*, Vol. 225, 2012, p. 101–106
- [18] M. O. Shabani, A. Mazahery: *Materiali in Tehnologije*, Vol. 46, 2012, p. 109–113
- [19] R. Hwang, Y. Chen, H. Huang: *Expert Systems with Applications*, Vol. 37, 2010, p. 3136–3139
- [20] L. Fratini, G. Buffa, D. Palmeri: *Computers and Structures*, Vol. 87, 2009, p. 1166–1174
- [21] R. Hamzaoui, M. Cherigui, S. Guessasm, O. ElKedim, N. Fenineche: *Materials Science and Engineering A*, Vol. 163, 2009, p. 17–21
- [22] N.S. Reddy, A.K. P. Rao, M. Chakraborty, B.S. Murty: *Materials Science and Engineering A*, Vol. 391, 2005, p. 131–140
- [23] A. Mazahery, M. O. Shabani: *JOM*, Vol. 64, 2012, p. 323-329.
- [24] F. Karimzadeh, A. Ebnonnasir A. Foroughi: *Materials Science and Engineering A*, Vol. 432, 2006, p. 184–190
- [25] N. Altinkok, R. Koker: *Materials and Design*, Vol. 25, 2004, p. 595–602
- [26] A. M. Hassan, A. Alrashdan, M. T. Hayajneh, A. T. Mayyas: *Journal of Materials Processing Technology*, Vol. 209, 2009, p. 894–899
- [27] S. K. Singh, K. Mahesh, A. K. Gupta: *Materials and Design*, Vol. 31, 2010, p. 2288–2295
- [28] P. J. Lisboa, A. F.G. Taktak: *Neural Networks*, Vol. 19, 2006, p. 408–415
- [29] M. O. Shabani, A. Mazahery, A. Bahmani, P. Davami, N. Varahram: *Kovove Materialy*, Vol. 49, 2011, p. 253-258
- [30] M. O. Shabani, A. Mazahery: *JOM*, Vol. 63, 2011, Vol. 132-316
- [31] A. Mazahery, M. O. Shabani: *Powder Technology*, Vol. 217, 2012, p. 558–565
- [32] A. Mazahery, M. O. Shabani: *Composites Part B*, Vol. 43, 2012, p. 1302-1308
- [33] D.P. Mondal, N.V. Ganesh, V.S. Muneshwar: *Materials Science and Engineering A*, Vol. 433, 2006, p.18-31
- [34] M. O. Shabani, A. Mazahery, M. R. Rahimpour, A. A. Tofigh, M. Razavi: *Kovove Materialy*, Vol. 50, 2012, p. 25-31
- [35] R.G. Reddy: *Review Advance Materials Science*, Vol. 5, 2003, p. 121-125
- [36] Y.C. Kang, S.L.I. Chen: *Chemical Physics*, Vol. 85, 2004, p. 438–443
- [37] E.M. Maik, O. Beort, S. Kleiner, U. Vogt: *Composite Science and Technology*, Vol. 679, 2007, p. 2377–2383
- [38] K.M. Mussert, W.P. Vellinga, A. Bakker, S. V. D. Zwaag: *Journal of Materials Science*, Vol. 37, 2002, p. 789-794
- [39] S.F. Hassan, M. Gupta: *Journal of Materials Science*, Vol. 41, 2006, p. 2229–2236
- [40] S.F. Hassan, M. Gupta: *Materials Science and Engineering A*, Vol. 392, 2005, p. 163–168

- [41] M. Gupta: *Wear*, Vol. 259, 2005, p. 620-625
- [42] H. Jones: *Wear*, Vol. 259, 2005, p. 577-589
- [43] Z. H. Di, L. Guobin: *Materials and Design*, Vol. 26, 2005, p. 454-458
- [44] A. T. Alpas, J. Zhang: *Wear*, Vol. 155, 1992, p. 83-104